DOI: 10.13009/EUCASS2023-004
Aerospace Europe Conference 2023 – 10TH EUCASS – 9TH CEAS

Earth atmosphere remnants as an electric propulsion propellant

Chloe Berenguer and Konstantinos Katsonis*†*
** DEDALOS Ltd*
Vassilissis Olgas 128, 54645 Thessaloniki, Greece
berenguer.dedalos@gmail.com – katsonis.dedalos@gmail.com
† Corresponding Author

Abstract

4CDGM, a volume averaged detailed global model with the four initial components O, O_2 , N, N_2 can analyse the functioning of air-breathing electric thrusters to foresee the plasma constitution and to diagnose it by OES.
4CDGM may also evaluate the atmospheric remnants in altitudes exceeding the Karman line set in about 100 km altitude on the basis of existing empirical models.
In order to support air-breathing thrusters, 4CDGM provides Plasma Component Composition diagrams, Functioning Diagrams and also theoretical spectra emission line intensities, thus allowing for OES diagnostics. Such diagrams and theoretical spectra are presented and discussed herewith.

1. Introduction

Evaluation of the Atmospheric Remnants (AtmRems) composition is mandatory if they are to be used as propellant of Electric Thrusters (ET) after their condensation. These ET are meant for propulsion of satellites in various altitudes and also of s/c involved in near Earth missions. The Four Component {N, N_2, O, O_2} Detailed Global Model (4CDGM) has been used for evaluating AtmRems in altitudes of 140 km - 260 km, for theoretical characterization of various types of electric thrusters fueled by AtmRems (see [1] and references therein) and also for non-intrusive diagnostics of the modeled thrusters [2]. In this case, 4CDGM provides the following support in an *In Situ* Resource Utilization (ISRU) scheme :
(I) Earth atmospheric composition analysis (see e.g. [3,4], DEDALOS Ltd report [5] and references therein).
(II) Evaluation of O_2/N_2 ratios to be used for ET fuelling in experiments meant to simulate the expected ET plasma when it is fed by AtmRems encountered in various altitudes [6].
(III) Characterization of various types of ETs [1,7,8] and references therein.
(IV) ET diagnostics based on Optical Emission Spectroscopy (OES) [7,9] and references therein.
Atmospheric composition in various altitudes is important not only when AtmRems are to be used as propellant, but also for satellite drag calculation and for re-entry studies. Besides composition, various characteristics of the atmosphere are important. It is to be noted that in a general way the thermosphere exhibits high temperatures (say from 600 K to 1400 K) and quite low pressures (e.g. of about 10^{-9} Atm at 200 km altitude).
As was the case previously [10], Low Earth Orbits (LEO), Very Low Earth Orbits (VLEO) [11] and Extremely Low Earth Orbits (ELEO) studies [12], providing support of ET development in case of fueling by AtmRems with ISRU in the lower thermosphere region, 4CDGM is also used as main tool in the present work. However, the presented and discussed examples concern specifically VLEO for lack of space. The obtained theoretical results for the considered ET with a given form factor are described and discussed by using:
- Standard Plasma Component Composition (PCC) diagrams [13,14], which illustrate the ET plasma composition. These diagrams give also the plasma electron temperature T_e and electron density n_e.
- Functioning Diagrams (FD) giving the plasma ionization percentage for the used propellant as a function of T_e , of the pressure p and of the absorbed power P_{ABS} . The isothermal, isoenergetic and isobaric curves composing the FDs illustrate the ET functioning.
- Theoretical atomic spectra including line intensities of the neutral and of the ionic oxygen and nitrogen species. 4CDGM can be used generally for any oxygen/nitrogen mixture study. Here, it results to theoretical intensities of the main O I and O II and also N I and N II lines. These are to be compared with the corresponding experimental ones in order to obtain non perturbing diagnostics based on OES of the ET plasma [2] in case of feed by AtmRems. Towards

DOI: 10.13009/EUCASS2023-004

this aim, the 4CDGM code incorporates detailed structure description of oxygen and nitrogen neutral and ionic species, including the necessary atomic and molecular data sets.

- Simplified feeding of prototypes designed for Air-Breathing Electric Thruster (ABET) propulsion experiments on ground by using calculated O_2 / N_2 gases mixtures as an alternative. Such mixtures, when used instead of the AtmRems mixture itself, can simulate the real AtmRems constitution which is encountered in the space at the selected altitude. Thus, beam-free laboratory simulation for ET prototypes in various conditions is obtained. Consequently, characterization, diagnostics and optimization of the ABET prototypes are much facilitated when using 4CDGM as support [6], because an adequate feeding by calculated O_2 / N_2 mixtures can simply replace the feeding by the expected AtmRems, which would require use of cumbersome hyperthermal atomic / molecular oxygen and nitrogen beams, experimental results for AtmRems feeding simulation can be obtained in a simpler way.

ISRU electric propulsion may in principle address the lower thermosphere region beginning from 100 km, where N_2 is the main constituent. Higher altitude regions, where atomic oxygen becomes the most present constituent, are also of interest. As was reported elsewhere [5], the NRL-MSISE-00 code, developed in Naval Research Laboratory [15], provides the necessary constitution, density and temperature values in the Earth thermosphere.

Fig. 1 illustrates the characteristics of the region of interest here, with N_2 and O becoming its main components, with the less present O_2 and N. Argon and helium appear in quite lower percentages and are neglected in the addressed ISRU thruster fueling scheme. This figure is obtained using results from the NRL-MSISE-00 code, specifically in case of mean and of high Solar and Geomagnetic (S&G) activities. It shows that besides presence of molecular nitrogen and atomic oxygen, molecular oxygen appears as considerable component only for lower altitudes, while atomic nitrogen presence almost vanishes when altitude diminishes to approach the Karman line limit at about 100 km. This reminds the ratio of the N_2/O_2 components percentage corresponding to the atmosphere at the sea level.

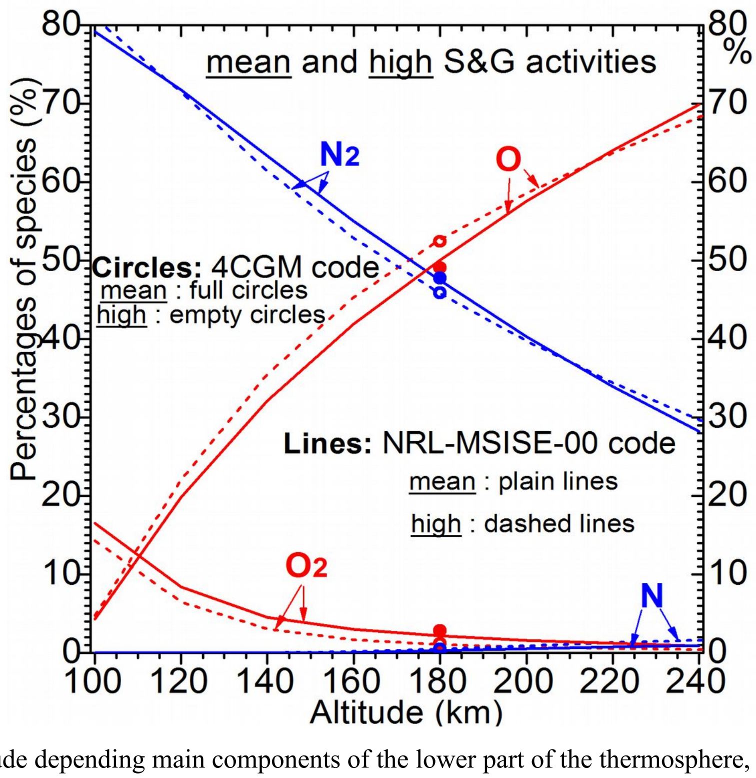

Figure 1. Altitude depending main components of the lower part of the thermosphere, 100 km to 240 km altitude

The small circles included in Fig. 1 show the results obtained from 4CDGM in case of 180 km altitude, with the nitrogen molecule presence taken as basis for mean (full circles) and for high (empty circles) S&G activities. Moreover, it has to be mentioned that, due to the lack of sufficient measurements, the electron, ion and neutral temperatures equilibrium expected in the lower part of the Fig. 1 altitudes is not yet well understood [16].

Results presented in the following sections concern specifically only the case of mean S&G activities, addressing fuelling by AtmRems in a region of about 180 km from the sea level, in case of moderate absorbed power of 0.8 kW to 2.5 kW.

Following this introduction, PCC diagrams together with their conjugate ones are presented and discussed in Section 2, allowing for characterizing ETs fueled by AtmRems. Typical examples of PCC results obtained by 4CDGM are given in this section. An evaluation of the ET functioning conditions is addressed and illustrated by means of a FD in Section 3. OES diagnostics using theoretical line intensities obtained simultaneously by 4CDGM is described and discussed in Section 4. Finally, Section 5 contains the main conclusions and perspectives of the present work.

DOI: 10.13009/EUCASS2023-004

2. 4CDGM modeling of interest to ABET

The plasma composition obtained by 4CDGM in case of P_{abs} = 1 kW is illustrated in Fig. 2. As was the case with previous results presented elsewhere [3,8], in order to ease the reading in Fig. 2 and following ones, densities of components containing only nitrogen are shown in blue, while those containing only oxygen are shown in red. Results concerning components which contain both nitrogen and oxygen atoms are not included in the figure in order to simplify the presentation, as molecular species are less abundant, even in this altitude.

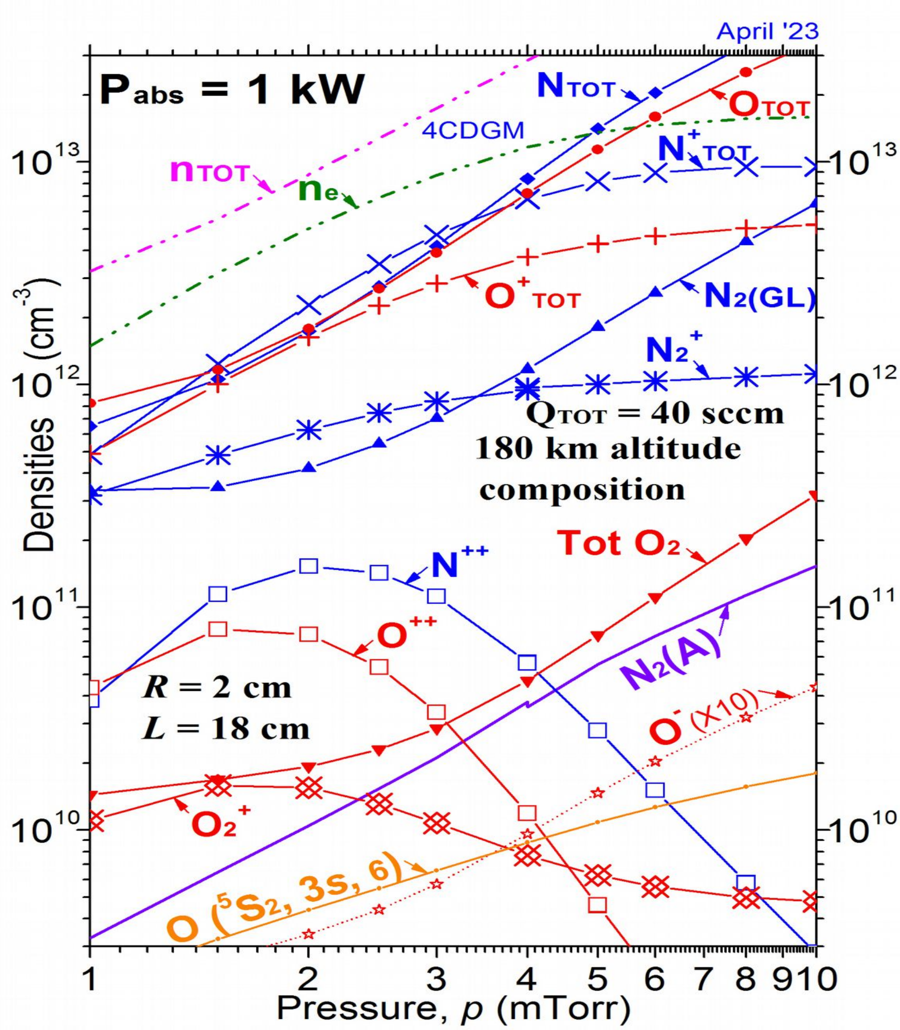

Figure 2. Pressure-dependent PCC, for 40 sccm AtmRems feed at 180 km altitude and 1 kW absorbed power. Form factor is *R*=2 cm, *L*=18 cm

In Fig. 2, pressure varies from 1 mTorr to 10 mTorr. Interesting variations of the constituents presence appear in this region. Note that curves present in these and in subsequent figures are used to ease the eye and symbols introduced in Fig. 2 are also used in subsequent diagrams. Figure 2 contains a PCC diagram providing fundamental results as total density n_{TOT} (dash double dotted magenta line), electron density n_e (dash double dotted green line) and the densities of the main plasma constituents. Note that electron temperature T_e values will be given in the conjugate diagram contained in Fig. 3.

Under the chosen conditions, n_e and consequently the sum of the ionic species densities, are high. It can be seen in Fig. 2, that n_e increases from about 1.5x10^{12} cm^{-3} for 1 mTorr to 1.6x10^{13} cm^{-3} for 10 mTorr although it has the tendency to reach a plateau after 6 mTorr.

Due to the relatively high P_{abs} of 1 kW, the most abundant species in the 1.5 mTorr to 3.5 mTorr region is the nitrogen ion. In the right part of the figure, we observe that the most abundant species shown are atomic nitrogen N_{TOT} (blue line with squares ♦) and atomic oxygen O_{TOT} (red curve with circles ●). The latter is already present in the propellant and the former is coming from the dissociation of the molecular nitrogen contained in the feed, of which the ground level N_2(GL) (blue line with full triangles ▲) remains abundant. The calculated n_e reflects the presence of

DOI: 10.13009/EUCASS2023-004

three different ionic species, namely atomic ion N^{+}_{TOT} (blue line with crosses x), atomic oxygen ion O^{+}_{TOT} (red line with crosses +) and molecular nitrogen ion N_2^+ (blue line with stars) reported following a diminishing order of their abundance values for all pressures. They bear rather similar values, sharing the total presence of positive ions which increase with pressure, to follow the aforementioned increase of n_e .
At the lower part of Fig. 2, presenting rather scarce species, appear the neutral oxygen molecule, Tot O_2 (red line with inverted triangles ▼) with the well known nitrogen metastable excited level compound $N_2(A)$ (violet line) following quite lower. As expected, the density of O_2^+ (red curve with crossed diamonds) is more than an order of magnitude lower than the density of N_2^+, with values slightly higher than 10^{10} cm^{-3} for low pressures and going down after 2 mTorr. In the same density region but quite lower, appear the metastable atomic oxygen species $O(^5S_2\ ,\ 3s)$ orange curve, where the number 6 refers to its order in the corresponding atomic oxygen Grotrian diagram.
Doubly ionized species are clearly present in view of the absorbed power value of 1 kW. Densities of N^{++} (blue line with hollow squares □) and of O^{++} (red line with hollow squares □) appear with values around 10^{11} cm^{-3} in the low left region of the Fig. 2. Besides, the electronegativity is found quite low, with the negative oxygen O^- (red dotted line with hollow stars) values multiplied by ten in order to be included in Figure 2.
A diagram concomitant to the PCC given in Fig. 2, showing in detail the variations of T_e (black curve with squares ■, values to be read at the left side of the figure) under the same conditions with those of Fig. 2 is presented in the following Fig. 3. Also represented in this figure are species percentages (of blue and red curves for nitrogen and oxygen species respectively), ionization percentage ξ_{TOT} (green curve with full circles ●) and electron percentage n_e / n_{TOT} (green curve with hollow circles ○), with values to be read at the right side of the figure. We observe in this figure that T_e reaches more than 30 eV for a pressure of 1 mTorr.

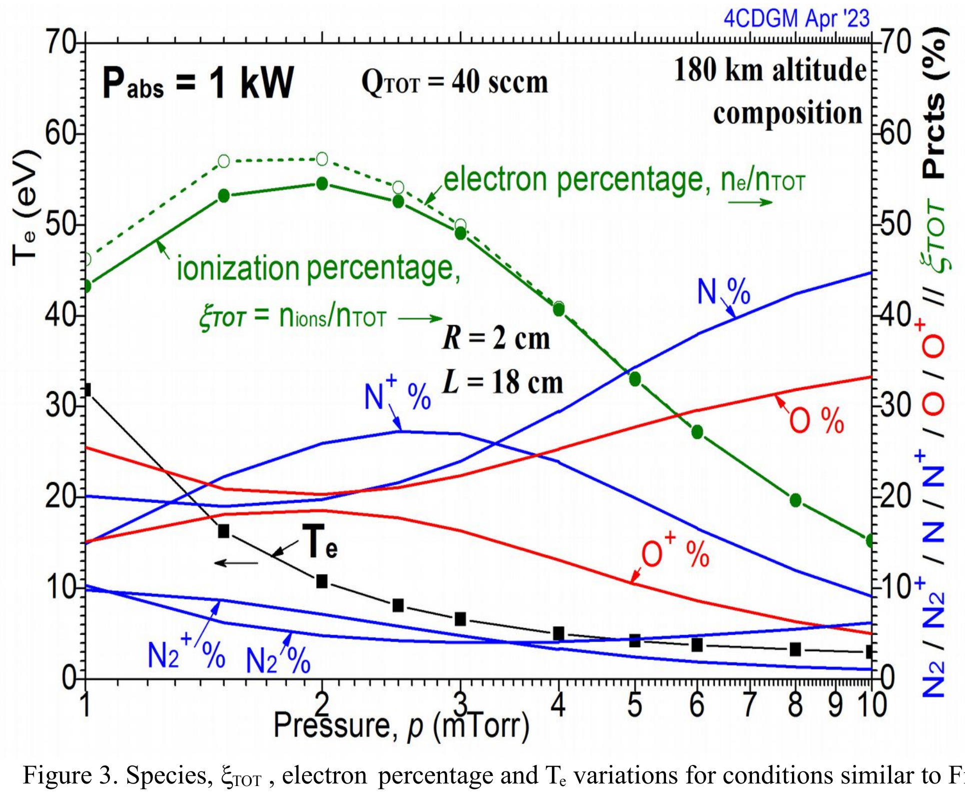

Figure 3. Species, ξ_{TOT} , electron percentage and T_e variations for conditions similar to Fig. 2

ξ_{TOT} values decrease regularly with increasing pressure, going down to about 15 % for 10 mTorr after increasing from 43 % for 1mTorr to around 55 % for 3 mTorr. It can also be seen in Fig. 3 that the electron percentage is higher than the ionization percentage for low pressure values, which however is calculated following the total number of ions without distinction of each species charge. This indicates the presence of doubly ionized species in this pressure region.
In case of higher absorbed power the observed plasma ionization appears clearly increased, with all the constituents presence modified. As an example, we address a power absorption of P_{abs} = 1.5 kW. The plasma composition obtained by 4CDGM in this case is illustrated by the PCC shown in Fig. 4. In this figure, pressure varies also from 1 mTorr to 10 mTorr, with interesting variations of the constituents presence appearing. In the PCC diagram presented in Fig. 4, fundamental results as total density n_{TOT} , electron density n_e and consequently the sum of the ionic species

DOI: 10.13009/EUCASS2023-004

densities have higher values than in case of P_{abs} = 1 kW, notably for higher pressure values. The corresponding electron temperature T_e values are also given in the conjugate diagram contained in Fig. 5.

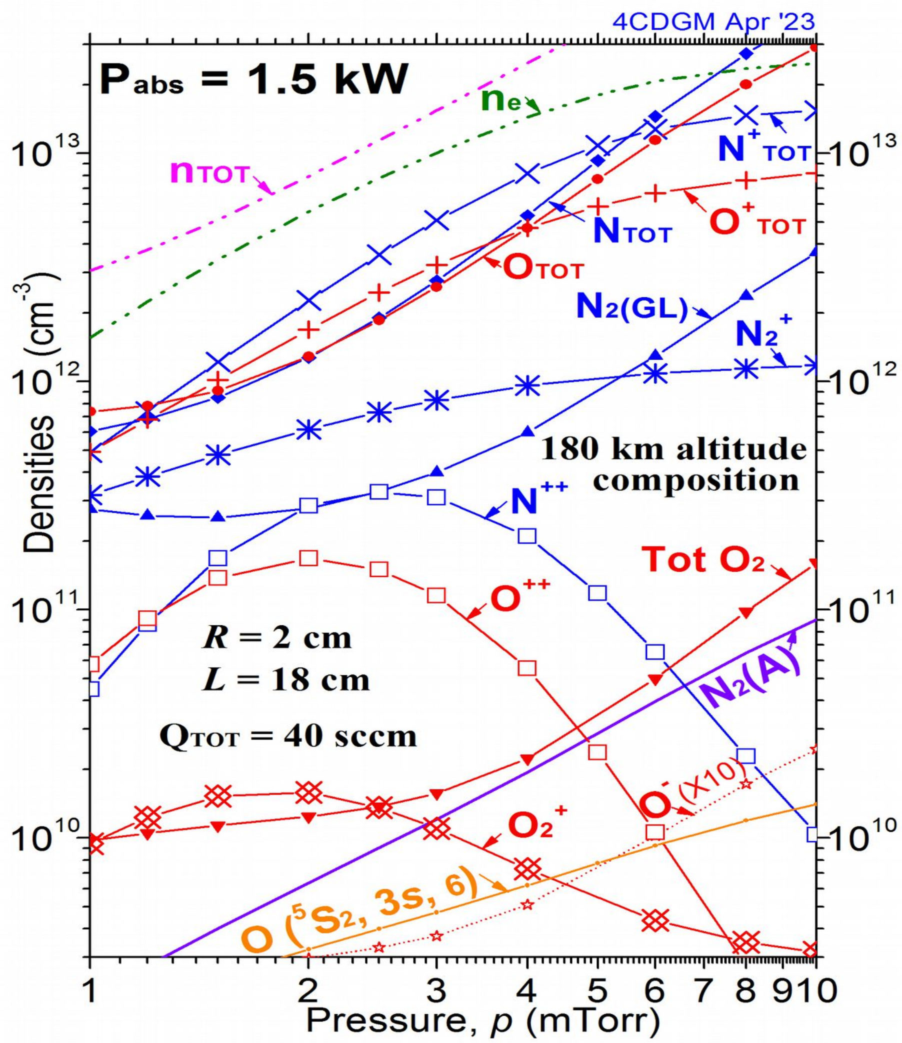

Figure 4. Pressure-dependent PCC, for 40 sccm AtmRems feed at 180 km altitude and 1.5 kW absorbed power. Form factor is *R*=2 cm, *L*=18 cm

It can be seen in Fig. 4, that n_e increases from about 1.6x10^{12} cm^{-3} for 1 mTorr to 2.5x10^{13} cm^{-3} for 10 mTorr, although this increase is slower for higher pressure values. The most abundant ionized species are again the nitrogen ion N^+_{TOT} and the oxygen ion O^+_{TOT} , but they show often higher densities than the neutral components due to the higher P_{abs} value of 1.5 kW. However, for high pressure values we observe that the most abundant species shown are still the atomic nitrogen N_{TOT} and the atomic oxygen O_{TOT} . The ground level N_2(GL) is less abundant because the dissociation has increased. Consequently, the N_2^+ densities increase much slower than the N^+_{TOT} and O^+_{TOT} ones. The doubly ionized species N^{++} and O^{++} have increased densities, due to the increased P_{abs} value, while the Tot O_2 presence is lower.

A diagram concomitant to the PCC given in Fig. 4, showing in detail the variations of T_e (black curve with squares ■, values to be read at the left side of the figure) under the same conditions with those of Fig. 4 is presented in the following Fig. 5. Also represented in this figure are species percentages (of blue and red curves for nitrogen and oxygen species respectively), ionization percentage ξ_{TOT} (green curve with full circles ●) and electron percentage n_e / n_{TOT} (green curve with hollow circles ○), with values to be read at the right side of the figure as was the case with Fig. 3. We observe in this figure that T_e reaches more than 40 eV for a pressure of 1 mTorr.

ξ_{TOT} values increase in the 1 mTorr to 2 mTorr region, and thereafter decrease regularly with increasing pressure for higher pressures, going down to about 25 % for 10 mTorr from more than 60 % for 2 mTorr. It can also be seen in Fig. 5 that the electron percentage is quite higher than the ionization percentage for low pressure values, even it is calculated following the total number of ions n_{ions} , without distinction of each species charge. This indicates an increased presence of doubly ionized species in this pressure region.

DOI: 10.13009/EUCASS2023-004

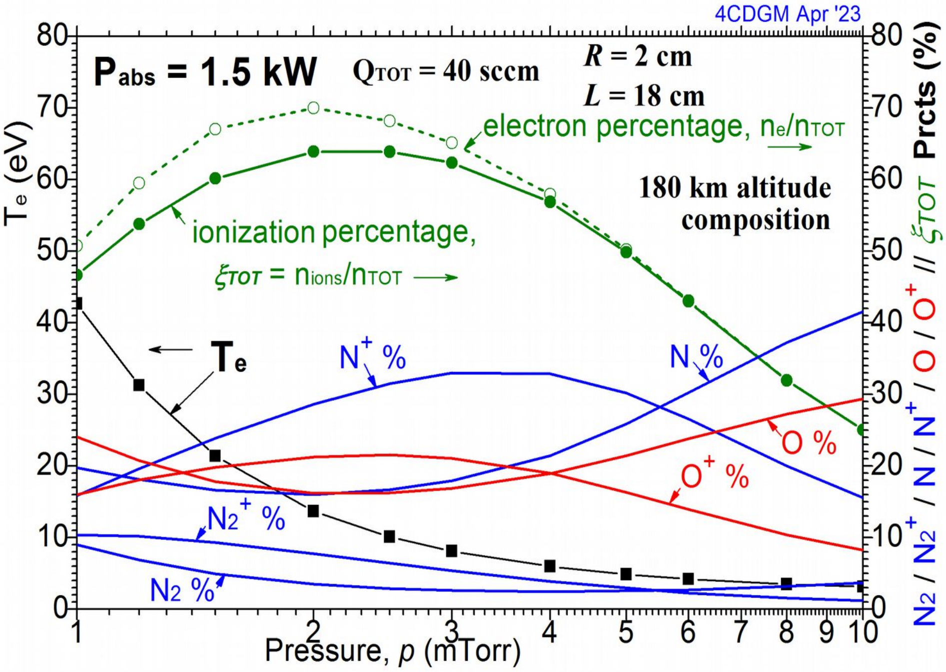

Figure 5. Species, ξ_{TOT} , electron percentage and T_e variations for conditions similar to Fig. 4

3. ET functioning

Percentages of the plasma components ionization are important for the obtaining of sufficient thrust. They are presented in the next Fig. 6, following isoenergetic and isothermal curves with pressure as abscissa.
Results illustrated previously in the PCC diagrams of Figs. 2 and 4 and similar ones, which provide snapshots of the plasma composition under various absorbed power values always with the same AtmRems feed value of 40 sccm, have been used in order to obtain the FD diagram shown in Fig. 6. This diagram gives a condensed description of the ET functioning.
Form factor addresses a cylinder with radius R of only 2 cm and of length L of 18 cm, as was the case in Section 2 and pressure spans a region extended from 1 mTorr to 10 mTorr as before. Characteristics of PCCs like these shown in Figs. 2 and 4 but also similar ones with different absorbed power values (0.8 kW, 1.3 kW, 2 kW, 2.5 kW) are embedded in Fig. 6.

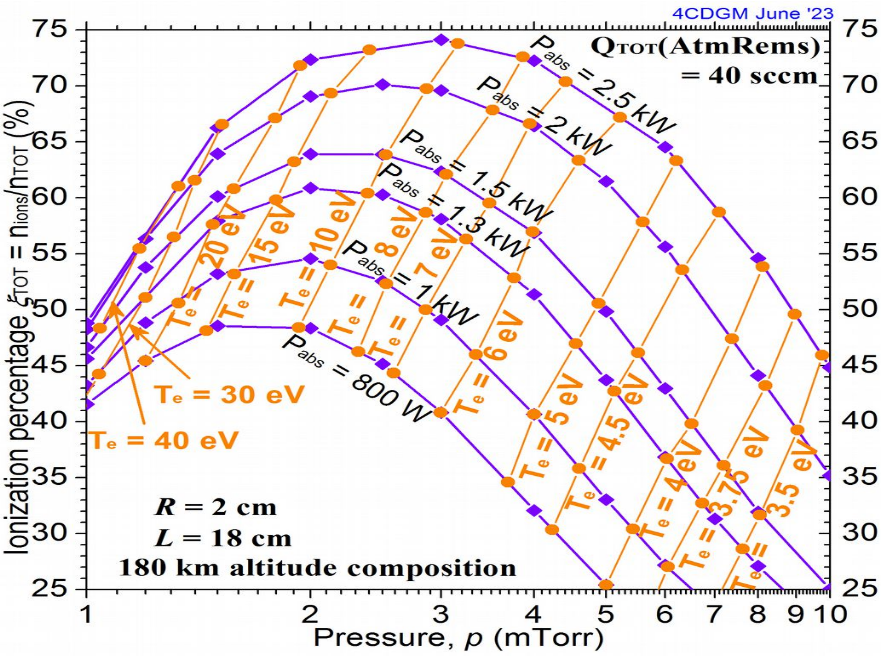

Figure 6. Pressure-dependent FD for 0.8 kW to 2.5 kW absorbed power. Form factor as in Figs. 2 to 5

DOI: 10.13009/EUCASS2023-004

The considered P_{abs} values allow for pressure dependent T_e values going from 3.5 eV up to 40 eV. We observe that for P_{abs} of about 1 kW, a satisfactory ionization of almost 55 % is obtained for pressures around 2.0 mTorr. In case of lower P_{abs} values, the provided power is mostly spent to chemical reactions, instead of increasing the ionization percentage [1].
It can also be seen in Fig. 6 that, once the propellant feed is selected (here Q_{TOT} = 40 sccm), the ionization level depends on the total pressure and on the absorbed power. It is to be noted that, as we address here an ISRU type technology, the availability of the propellant could become an important issue only in case of projects addressing High Earth Orbits (HEO) and of interplanetary missions, where resources *in situ* become scarce.

4. Optical emission spectroscopy diagnostics based on the calculated theoretical line intensities

Besides the modeling results described in the previous sections, 4CDGM supports non-intrusive OES diagnostics based in the obtained calculated theoretical spectral line intensities. When emission line intensities are acquired experimentally *in situ*, the plasma temperature and electron density can be diagnosed by comparison of the experimental with the theoretical values. As an example, theoretical spectra obtained by 4CDGM belonging to the most ionized plasma case presented in Section 2 with absorbed power of 1.5 kW described by the PCC of the Fig. 4, are presented and discussed in this section.
As was reported previously [3,8,12], it is possible to choose between neutral oxygen and nitrogen atoms spectra and the spectra of their ions as a basis of OES, with the most abundant species in the chosen conditions constituting in principle the best choice. Fig. 4 shows that for P_{abs} = 1.5 kW, the densities of N and N^+ are higher than those of O and O^+ for all the addressed pressure values. This is the contrary of what is often the case for LEO and for VLEO propulsion. However, in propulsion for VLEO, especially for low absorbed power values, this could not be the case, see e.g. [8].
We address first the case of OES diagnostics based on the nitrogen species, with this choice limited to its first and second spectra. Theoretical intensities in an extended wavelength λ region were calculated. This choice allows also to compare results from neutral N atoms with those coming by 4CDGM from N^+. The n_e and T_e results obtained by OES diagnostics based in the two nitrogen spectra can be further compared to those coming from OES based in oxygen ones.
The theoretical N spectrum obtained by 4CDGM for an absorbed power of 1.5 kW and a pressure of 2 mTorr is presented in the following Fig. 7, which contains spectral lines in the VUV, visible and IR regions.

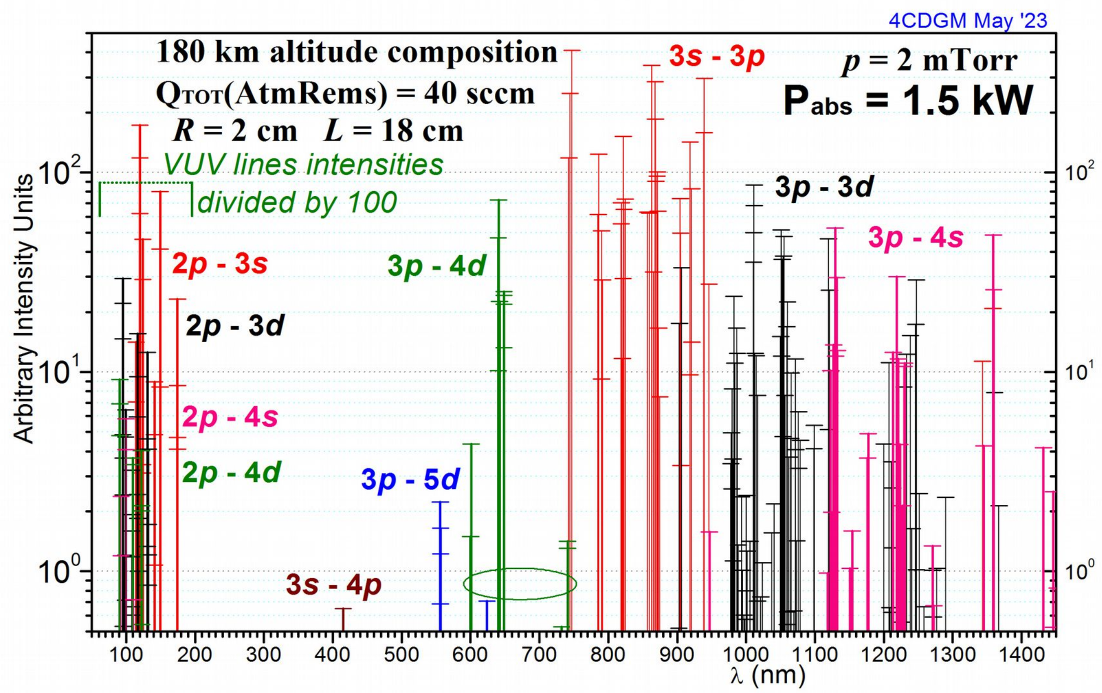

Figure 7. Extended N I spectrum in the VUV, visible and IR regions for 180 km altitude atmospheric composition for an absorbed power of P_{abs} = 1.5 kW

The main spectral lines are presented using different colors for the identification of the addressed multiplets and of the corresponding evaluated intensities, aiming a better distinction of the spectral components.

DOI: 10.13009/EUCASS2023-004

Calculated intensities shown in Fig. 7 corresponding to the VUV region are two orders of magnitude higher than those corresponding to the visible and IR regions of the figure. Therefore, they have been multiplied by 100 to include them in the figure. However, using of the UV, visible and near infrared lines is proposed for the OES, because the necessary experimental facilities are easier to handle.

By comparison of the N I theoretical line intensities shown in Fig. 7 with the corresponding experimental ones it becomes possible to obtain straightforwardly the corresponding values of T_e and n_e .

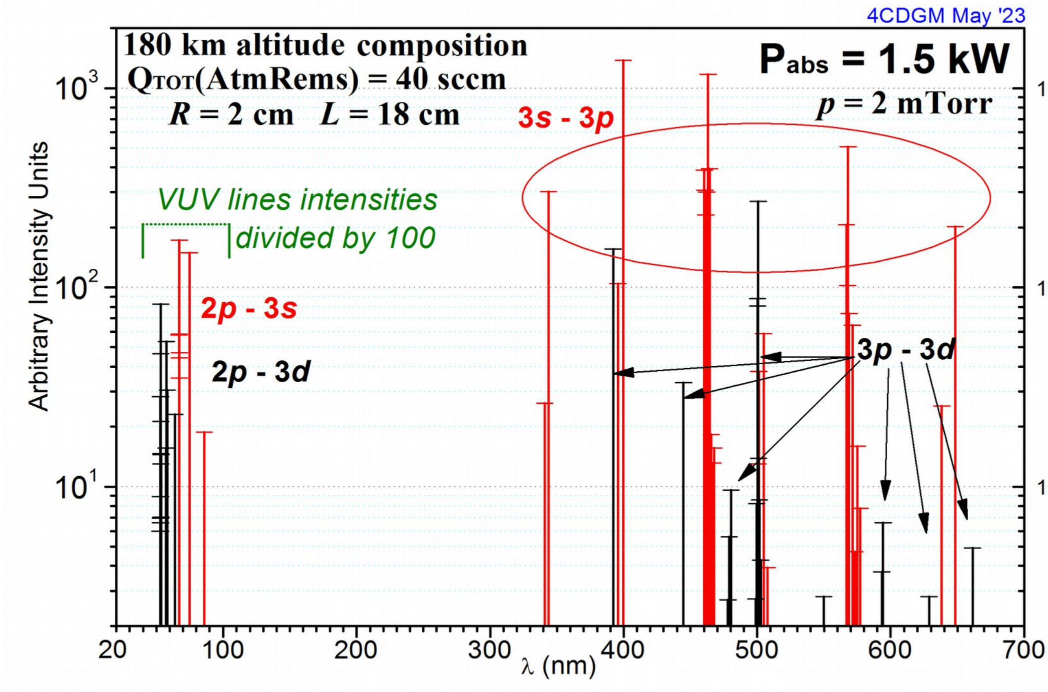

Figure 8. As in Fig. 7, but for N II theoretical spectrum

The main lines of the theoretical N II spectrum obtained by 4CDGM in the VUV, visible and IR regions for the same conditions with those of Fig. 7 are shown in Fig. 8, where the VUV lines intensities have also been divided by 100.

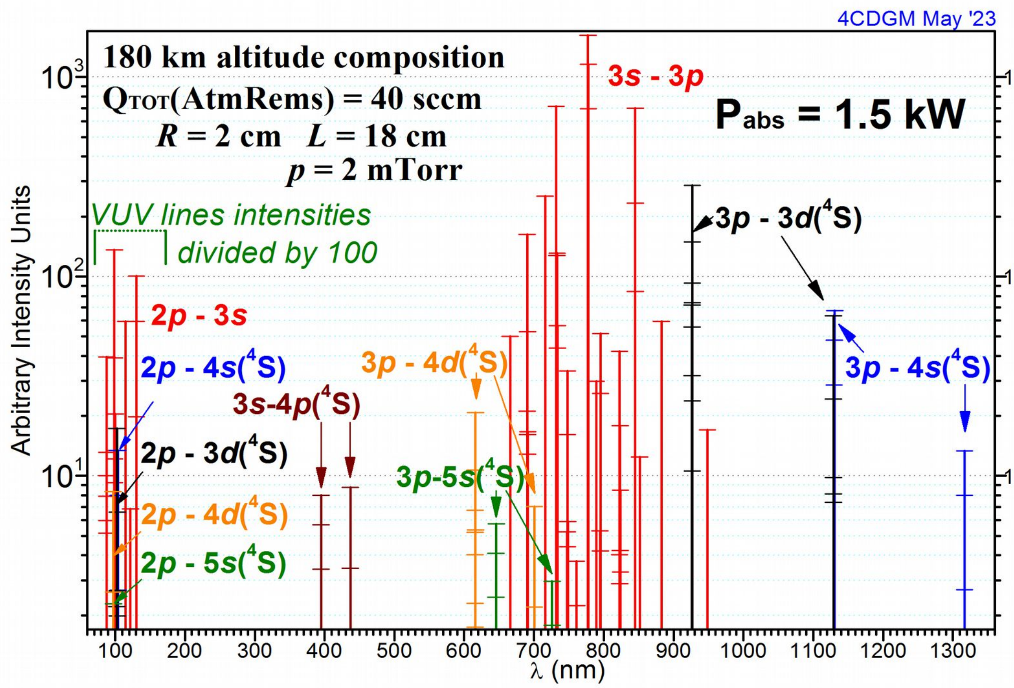

Figure 9. Extended O I spectrum in the VUV, visible and IR regions for 180 km altitude atmospheric composition for an absorbed power of P_{abs} = 1.5 kW

DOI: 10.13009/EUCASS2023-004

In addition to using the nitrogen species for OES diagnostics it is also possible to address the O, O^+ species and hence obtain the plasma ionization and electron temperature in a way analogous to the previous case. When the O, O^+ experimental intensities of emission lines are acquired, evaluations of n_e and T_e become possible, as 4CDCM provides also the theoretical intensities of the oxygen lines.
OES diagnostics based on the oxygen spectral line intensities is using the calculated ones shown schematically in the following Figs. 9 and 10. These figures pertain correspondingly to the first and the second oxygen spectra.
Note that the intensities of the VUV lines in both O I and O II spectra are also orders of magnitude higher than these pertaining to the VUV and visible / IR regions and their intensities are again divided by 100 in order to fit in the figures.

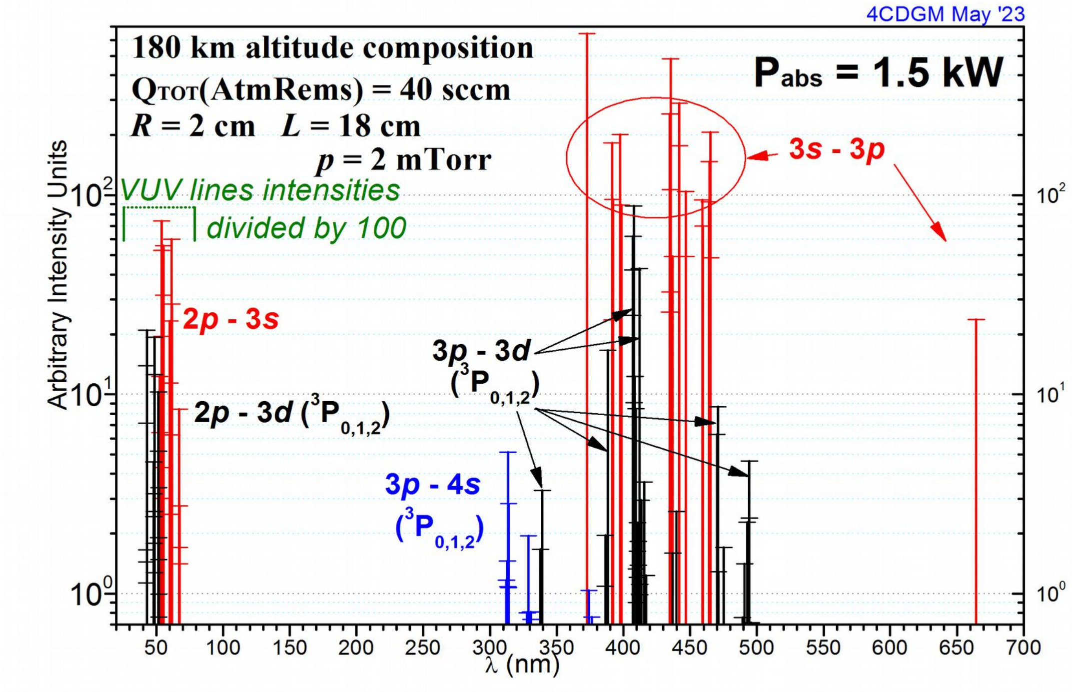

Figure 10. As in Fig. 9, but for O II theoretical spectrum

Even if the intensities of the resonant lines in the VUV regions are far more intense, the UV / visible / IR are traditionally used as a basis of the OES diagnostics, as was the case with the nitrogen based OES diagnostics.

5. Conclusions and perspectives

Using of AtmRems as propellant has been proposed in early LEO studies, see e.g. [17]. More recently, the 4CDGM model has been used as support in LEO and VLEO studies, see e.g. [9,10]. This model supports ISRU when AtmRems components are used as electric propulsion propellant. It also provides beam-free laboratory simulation for ET prototypes fueled with such propellants. DGMs for modeling, characterization and OES diagnostics of various other atmospheric propellants as those available in Venus, Mars [8] and Ice Giants [18] have been also made available. The possibility of installing satellites revolving in ELEOs has been addressed recently in [12]. In this paper, results obtained by 4CDGM concerning propulsion in the VLEO region have been presented and discussed using standard PCC and FD diagrams. Altitude of 180 km is taken as an example, with the AtmRems used as propellant constituted by about 50.1 % O, 47.5 % N_2 , 2.16 % O_2 and 0.28 % N in case of mean S&G activities. Note that Fig. 2 and even more Fig. 4 show that the presence of nitrogen inside the thruster is higher than this of the oxygen in case of 1 kW and 1.5 kW. Then, the expected erosion concerning ISRU type thrusters to be used in the selected altitude is lower than this encountered in the LEO case.
OES diagnostics is also addressed. This diagnostics becomes possible by using 4CDGM in order to calculate the theoretical spectral lines intensities valid for any initial conditions chosen. Consequently, both nitrogen and oxygen species theoretical spectra have been presented.
4CDGM results which are illustrated here, show that this model constitutes a strong support to the ISRU type ABET propulsion and specifically in the VLEO region.

References

[1] Berenguer, Ch. and Katsonis, K. (2023). *Atmospheric remnants as propellant for space electric propulsion*, EPIC 2023 Workshop, Naples, Italy, May 2023

DOI: 10.13009/EUCASS2023-004

[2] Berenguer, Ch., Katsonis, K., Gonzalez del Amo, J. and Stavrinidis, C. (2016). *Diagnostics of Air-Breathing Electric Thrusters by Optical Emission Spectroscopy*, 5th Space Propulsion Conference, Paper ID SP2016_**3124973**, Rome, Italy, May 2016

[3] Berenguer, Ch. and Katsonis, K. (2021). *Evaluation of Earth Atmosphere Remnants Used as Propellant in Electric Thruster Technology*, 7th Space Propulsion 2020+1 Conference, SP2020_**018**, Estoril, Portugal, March 2021

[4] Katsonis, K., Berenguer, Ch., Gonzalez del Amo J. and Stavrinidis, C. (2015). *Atmospheric Remnants in the Low Earth Orbit Region around 200 km Altitude*, World Journal of Engineering and Technology **3**, p. 26, October 2015

[5] Katsonis, K. and Berenguer, Ch. (2023). *Review of the Atmospheric Propellants*, Report DEDA-AETH-PD-**0204** Issue 1.3, Thessaloniki, Greece, March 5, 2023

[6] Katsonis, K., Berenguer, Ch. and Gonzalez del Amo, J. (2015). *Characterization of Air Breathing Plasma Thrusters Fuelled by Atmospheric Mixtures Encountered in Earth Atmosphere at an Altitude of About 200 km*, 34th International Electric Propulsion Conference, IEPC-2015-**268**, Kobe, Japan

[7] Berenguer, Ch., Katsonis, K. and Gonzalez del Amo, J. (2018). *Air Breathing Electric Thruster Characterization and Diagnostics by a Four Components Detailed Global Model*, 6th Space Propulsion Conference, Paper ID SP2018_**345**, Seville, Spain, May 2018

[8] Katsonis, K., Berenguer, Ch. and Cesaretti, G. (2020). *ISRU Technology Propulsion for Missions in the Solar System*, 1st Aerospace Europe Conference 2020, AEC2020_**523**, Bordeaux, France, 25 to 28 February 2020

[9] Berenguer, Ch. and Katsonis, K. (2018). *Characterization and Optical Diagnostics of Air – Breathing Electric Thrusters by 4CDGM*, EPIC 2018 Workshop, London, UK, October 2018

[10] Andreussi, T., Ferrato, E., Paissoni, C.A., Kitaeva, A., Giannetti, V., Piragino, A., Schäff, S., Katsonis, K., Berenguer, Ch., Kovacova, Z., Neubauer, E., Tisaev, M., Karadag, B., Lucca Fabris, A., Smirnova, M., Mingo, A., Le Quang, D., Alsalihi, Z., Bariselli, F., Parodi, P., Jorge, P. and MaginT.E. (2022). *The AETHER Project: Development of airbreathing electric propulsion for VLEO missions*, 1st International Symposium on Very Low Earth Orbit Missions and Technologies, CEAS Space Journal, https://doi.org/10.1007/s12567-022-00442-3, March 2022

[11] Katsonis, K. and Berenguer, Ch. (2021). *Modeling and Optical Diagnostics of Air-breathing Thrusters of 1 kW Class in Very Low Earth Orbit Missions*, 1st International Symposium on VLEO Missions and Technologies, Manchester, UK and virtual, June 2021

[12] Katsonis, K., Berenguer, Ch. and Gonzalez del Amo J. (2022). *Electric Propulsion for Extremely Low Earth Orbits*, SP2022_**041**, 8th Space Propulsion Conference, Estoril, Portugal, May 2022

[13] Berenguer, Ch. and Katsonis, K. (2022). *Modeling and Diagnostics of ISRU Technology Electric Thrusters meant for Extremely Low Earth Orbits Propulsion*, EPIC 2022 Workshop, Cologne, Germany, 4 - 8 April 2022

[14] Katsonis, K. and Berenguer, Ch. (2014). *Properties of the Atmospheric Mixtures Prevailing around 200 km Altitude in Conditions of Low Absorbed Power and Pressure*, 6th ESA RHTG Workshop, St. Andrews, UK, November 2014

[15] Picone, J.M., Hedin, A.E., Drob, D.P. and Aikin, A.C. (2002). *NRL-MSISE-00 Empirical Model of the Atmosphere: Statistical Comparisons and Scientific Issues*, J. Geophys. Res. **107**, 1468

[16] Peterson, W.K., Maruyama, N., Richards, P., Erickson, P.J., Christensen, A.B. and Yau, A.W. (2023). *What is the altitude of thermal equilibrium?*, Geophysical Research Letters **50** e2023GL102758, https://doi.org/10.1029/2023GL102758

[17] Di Cara, D., Gonzalez del Amo, J., Santovincenzo, A., Carnicero Dominguez, B., Arcioni, M., Caldwell, A. and Roma, I. (2007). *RAM Electric Propulsion for Low Earth Orbit Operation: an ESA Study*, 30th IEPC Conference, IEPC-2007-**162**, Florence, Italy, September 2007

[18] Berenguer, Ch., Katsonis, K. and Gonzalez del Amo, J. (2022). *Using the Constituents of the Giant Planets Atmospheres as ISRU Propellants for Electric Thrusters*, SP2022_**079**, 8th Space Propulsion Conference, Estoril, Portugal, May 2022